Research Article

Rapid Communications in Mass Spectrometry

Received: 28 September 2011 Revised: 2 December 2011 Accepted: 5 December 2011 Published online in Wiley Online Library

Rapid Commun. Mass Spectrom. **2012**, *26*, 449–459
(wileyonlinelibrary.com) DOI: 10.1002/rcm.6124

Application of the N_2/Ar technique to measuring soil-atmosphere N_2 fluxes

Wendy H. Yang* **and Whendee L. Silver**

Ecosystem Sciences Division, Department of Environmental Science, Policy, and Management, 130 Mulford Hall #3114, University of California, Berkeley, CA 94720, USA

RATIONALE: The emission of dinitrogen (N_2) gas from soil is the most poorly constrained flux in terrestrial nitrogen (N) budgets because the high background atmospheric N_2 concentration makes soil N_2 emissions difficult to measure. In this study, we tested the theoretical and analytical feasibility of using the N_2/Ar technique to measure soil-atmosphere N_2 fluxes.

METHODS: Dual inlet isotope ratio mass spectrometry was used to measure $\delta Ar/N_2$ values of gas sampled from surface flux chambers. In laboratory experiments using dry sand in a diffusion box, we induced a known steady-state flux of N_2, and then measured the change in the N_2/Ar ratio of chamber headspace air samples to test our ability to reconstruct this flux. We m\odeled solubility, thermal, and water vapor flux fractionation effects on the N_2/Ar ratio to constrain physical effects on the measured N_2 flux.

RESULTS: In dry sand, an actual N_2 flux of 108 mg N m^{-2} day^{-1} was measured as 111 $\pm$ 19 mg N m^{-2} day^{-1} ($\pm$ standard error (SE)). In wet sand, an actual N_2 flux of 160 mg N m^{-2} day^{-1} was measured as 146 $\pm$ 20 mg N m^{-2} day^{-1} when solubility and water vapor flux fractionation were taken into account. Corrections for thermal fractionation did not improve estimates of N_2 fluxes.

CONCLUSIONS: We conclude that our application of the N_2/Ar technique to soil surface fluxes is valid only above a detection limit of approximately 108 mg N m^{-2} day^{-1}. The N_2/Ar method is currently best used as a validation tool for other methods in ecosystems with high soil N_2 fluxes, but, with future improvements, it holds promise to provide high-resolution measurements in systems with low soil N_2 fluxes. Copyright © 2012 John Wiley & Sons, Ltd.

Soil dinitrogen (N_2) emissions represent the loss of nitrogen (N) from the biosphere to the atmospheric pool, thus completing the N cycle. Despite the importance of this flux, terrestrial ecosystem N budgets often do not include it[1,2] because it is difficult to measure against the high background atmospheric N_2 concentration.[3] In terrestrial ecosystems, N_2 is primarily produced via denitrification, a process by which nitrate (NO_3^-) is reduced to nitrous oxide (N_2O) and then subsequently to N_2. Nitrous oxide is a potent greenhouse gas and a catalyst for stratospheric ozone depletion. Thus, the relative amounts of N_2O and N_2 released to the atmosphere via denitrification can have major implications for atmospheric chemistry. Humans have drastically increased the amount of reactive N in the environment, stimulating soil N_2O emissions.[4] However, the effect of anthropogenic N loading on soil N_2 emissions is largely unknown.[5,6] In most managed ecosystems, N inputs greatly exceed the measured outputs, suggesting that a large amount of anthropogenic N is either stored in the ecosystem or released as N_2.[7] Accurate measurements of soil N_2 emissions are needed to better constrain ecosystem N budgets, elucidate controls on denitrification, and provide the data necessary to validate and improve models that predict ecosystem N losses as N_2O and N_2 emissions.[8]

A wide range of approaches has been used to estimate soil N_2 emissions, but each approach has well-recognized limitations.[3] Acetylene (C_2H_2) inhibits the reduction of N_2O to N_2 via denitrification. Thus, N_2 emissions can be estimated from the difference in N_2O production in the presence and absence of C_2H_2. The C_2H_2 inhibition technique can underestimate N_2 emissions by decreasing the supply of NO_3^- substrate via nitrification, through diffusion limitation of C_2H_2 to microsites of denitrification activity, and due to the ineffectiveness of C_2H_2 on some denitrifiers and under low NO_3^- conditions.[9,10] The addition of ^{15}N-labeled NO_3^-, the substrate for denitrification, can be used to trace the rate of NO_3^- reduction to N_2. The use of this method is typically restricted to systems with high soil NO_3^- concentrations, such as agricultural systems,[11] because a large amount of $^{15}NO_3^-$ is needed to detect a change in the ^{15}N enrichment of the atmospheric N_2 pool. This approach can potentially stimulate, and thus overestimate, denitrification rates as well as change the relative amounts of N_2O and N_2 produced. The gas flow soil core method has been used to estimate N_2 emissions from intact soil cores.[12,13] While this method has been successfully applied in a laboratory setting, the technical requirements make this method impractical in a field setting.[14] Finally, attempts have been made to characterize the N_2/N_2O ratio of denitrification

* *Correspondence to:* W. H. Yang, Ecosystem Sciences Division, Department of Environmental Science, Policy, and Management, 130 Mulford Hall #3114, University of California, Berkeley, CA 94720, USA.
E-mail: wendy_yang@berkeley.edu

end-products for specific study sites so that soil N_2 emissions can be estimated from soil N_2O emissions alone, which are relatively easy to measure with high resolution.[15,16] However, the N_2/N_2O ratios are often highly variable[13] and dependent on environmental conditions,[17,18] resulting in large uncertainty in estimates of soil N_2 emissions derived by this method.[2]

Several recent advances have contributed to our understanding of soil N_2 emissions. First, ^{15}N isotope budgets can be used to constrain gaseous N losses based on mass balance models and, with measurements of NO_x losses, soil N_2 emissions can be estimated at the ecosystem scale[19] and at the global scale.[20] This method integrates over time and space to avoid the need for high-resolution measurements of soil N_2 emissions but, as a result, it cannot provide insights into smaller scale patterns in emissions within ecosystems or with changing environmental conditions. Second, the $^{15}N_2O$ pool dilution method provides field measurements of gross N_2O production and consumption that can be related to soil characteristics, such as soil O_2 and mineral N concentrations.[21] Because this method measures N_2O consumption from the loss of $^{15}N_2O$ tracer, it may not capture complete denitrification that occurs intracellularly. Thus, the measured N_2O consumption rates may only be an index of soil N_2 emissions. These methods can be powerful tools for answering specific questions about N budgets or denitrification and, if used in conjunction with complementary methods that compensate for their limitations, can be used to answer a broader set of questions about denitrification to N_2 and the controls on the N_2O:N_2 ratio.

All the methods presented thus far, except for the gas flow soil core technique, specifically measure N_2 production via denitrification, but recent studies suggest that there may be other important terrestrial N_2 production pathways. In marine and freshwater ecosystems, anaerobic ammonium (NH_4^+) oxidation using nitrite (NO_2^-) as an electron acceptor (termed anammox) accounts for up to 67% of N_2 production.[22–24] Anammox has not been demonstrated to occur in soils,[25] but the Planctomycetes responsible for anammox have been detected in soils.[26,27] Recently, the production of N_2 by iron (Fe) reduction coupled to anaerobic NH_4^+ oxidation was demonstrated in humid tropical forest soils.[28] This process, termed Feammox, may be important in highly weathered soils rich in poorly crystalline Fe. Thus, methods that specifically measure N_2 production via denitrification could underestimate gross N_2 production, but they would remain useful for studying rates of and controls on denitrification.

The N_2/Ar technique is used widely in aquatic systems to measure net N_2 production, but is more challenging to apply in terrestrial ecosystems. This method uses argon (Ar), an inert gas, as a conservative tracer. Thus, measured changes in measured N_2/Ar ratios can be attributed to changes in the abundance of N_2. Membrane inlet mass spectrometry (MIMS) can be used to measure N_2/Ar ratios with high throughput (20–30 samples per hour) and with 0.05% precision (in terms of coefficient of variation) so that N_2 fluxes as low as 0.7 mg N m^{-2} day^{-1} can be measured.[29] The N_2/Ar technique is more challenging to apply in terrestrial ecosystems because higher precision is necessary to detect changes in the N_2/Ar ratio in air. The concentration of N_2 in air is approximately 50 times more than that at saturation in fresh water at 20 °C. In addition, soils on average exhibit 10 times lower denitrification rates than aquatic sediments.[30] These factors together suggest that minimum detectable soil N_2 fluxes are approximately 500 times lower than minimum detectable sediment N_2 fluxes, and that MIMS does not have the precision to detect changes in N_2/Ar ratios from soil gas fluxes. Paleoclimatologists have developed an analytical approach to measure N_2/Ar ratios with per meg level precision (i.e., 10^{-3} per mil) by using isotope ratio mass spectrometry (IRMS) to reconstruct past climate from ice core bubbles.[31] In addition, expected changes in the N_2/Ar ratio due to soil N_2 emissions are so small that physical fractionation effects on the N_2/Ar ratio that can confound estimates of soil N_2 emissions due to biological processes. In terrestrial ecosystems, these effects include thermal fractionation, solubility fractionation, and water vapor flux fractionation. Because these fractionation effects on the N_2/Ar ratio are governed by physical effects, they can be modeled to remove their confounding effect on measured shifts in N_2/Ar ratios.

In this paper, we present the theoretical considerations of the N_2/Ar approach for terrestrial N_2 fluxes and provide a preliminary test of the validity and accuracy of the N_2/Ar technique for measuring surface soil N_2 fluxes under controlled laboratory conditions. Our goal was to explore the theoretical and analytical feasibility of this approach. This is a necessary first step to determine if the approach holds promise prior to the significant effort involved in optimizing the method for deployment under real-world conditions. The objectives of this study were to determine a preliminary detection limit of the N_2/Ar method for soil fluxes and also to determine if observed changes in the N_2/Ar ratio can be corrected for physical fractionation effects. While we refer to this method as the 'N_2/Ar method' because N_2 is the gas of interest, when presenting methods and data, we will refer to $\delta Ar/N_2$ according to the tradition of expressing isotope ratios (or in this case, elemental ratios) with the heavier isotope in the numerator.

THEORY AND CALCULATIONS

Thermal fractionation

In the presence of a temperature gradient, a mixture of N_2 and Ar will become fractionated because the heavier molecule, Ar, tends to reside on the colder end of the gradient while the lighter molecule, N_2, tends to reside on the warmer end of the gradient.[32] This phenomenon is known as thermal diffusion.[33,34] Temperature changes during a surface flux measurement can affect the N_2/Ar ratio via thermal diffusion by disturbing the temperature gradient from the soil to the atmosphere. We assume that the soil column and air are at thermal steady state initially and that they reach a new steady state by the time of the final gas sampling. We define thermal steady state as one in which the gas composition has come into equilibrium with the soil temperature profile. Because gas diffusion is typically faster than heat diffusion in soils, this equilibrium can be approximately attained even if the temperature profile itself is not at steady state. Thus, the thermal fractionation effect (expressed as δ Ar/N_2 in units of per meg) can be calculated as the difference in the thermal diffusion effect at the initial and final sampling time points.

Rapid Communications in Mass Spectrometry

At each time point, the thermal diffusion effect (in per meg units), δ_d, can be calculated using the following equation,[35] where T_0 is the soil temperature at bottom of soil (K), T is the chamber air temperature (K), and α is the thermal diffusion factor for N_2/Ar (Eqn. (1)):

$$\delta_d = \left[\left({}^{T_0}/_{T}\right)^{\alpha} - 1\right] * 10^6 \quad (1)$$

We used an α-value of 0.078 for a mixture of N_2-Ar in atmospheric proportions at 293 K based on empirically determined values for different N_2-Ar mixtures and at different temperatures reported in the literature (see Supporting Information). This α-value translates to a thermal diffusion effect of 286 per meg per K.

Solubility fractionation

Temperature changes during surface flux measurements can also affect the N_2/Ar ratio because of the differing temperature-solubility curves for different gases dissolved in water (Fig. 1). We call this the solubility fractionation effect. Note that this is a transient solubility effect different from equilibrium solubility fractionation defined by geochemists. The magnitude of the solubility fractionation effect depends on soil moisture and the change from a given initial temperature (Fig. 2). For example, at 10% gravimetric soil moisture, up to 0.5 °C changes in temperature from 20 °C result in <50 per meg shifts in the N_2/Ar ratio. However, at 40% gravimetric soil moisture, the solubility fractionation effect is 100 per meg for every 0.1 °C change in temperature.

To estimate the solubility fractionation effect, we first calculated the proportion of soil that is particles (f_p), water (f_w), and air (f_a) from the gravimetric soil water content (θ, kg water kg soil^{-1}), bulk density (ρ_b, g cm^{-3}), and total soil porosity (P_T, m^3 voids m^{-3} soil) using Eqns. ((2))–((4)). The sum of f_p, f_w, and f_a must equal 1. Thus, in 1 m^3 of soil at standard temperature and pressure (STP), the amount of soil particles (n_p), water (n_w), and air (n_a) is equivalent to f_p, f_w, and f_a, respectively, in units of m^3 STP.

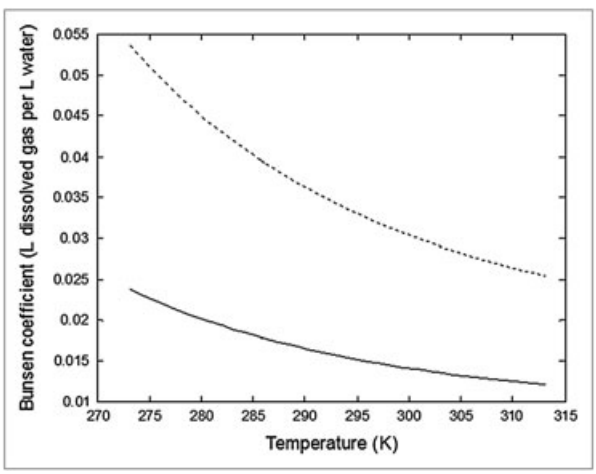

Figure 1. Temperature-solubility curves for N_2 (solid line) and Ar (dashed line). Bunsen coefficients were calculated from the fitting curves reported by Hamme and Emerson.[37]

$$f_w = \theta * \rho_b \quad (2)$$

$$f_a = P_T - f_w \quad (3)$$

$$f_p = 1 - P_T \quad (4)$$

The total porosity was calculated from ρ_b, 1.42 g cm^{-3}, and particle density (ρ_p, 2.55 g cm^{-3}) determined for the diffusion box sand used in this experiment[36] (Eqn. (5)).

$$P_T = 1 - \frac{\rho_b}{\rho_p} \quad (5)$$

Hamme and Emerson[37] made high-precision measurements of N_2 and Ar solubility in distilled water from 0 to 30 °C. We used their equations to calculate N_2 and Ar Bunsen coefficients (β, L of gas dissolved per L of water) at the temperatures measured when the initial and final gas samples were taken. We calculated the change in N_2 contained in soil water, $\Delta n_{N2,w}$, using Eqn. (6) where X_{N2} is the dry air mole fraction of N_2 (0.78084 m^3 STP N_2 m^{-3} STP) from Glueckauf:[38]

$$\Delta n_{N2,w} = \left(X_{N2} * \beta_{N2,final} * n_w\right) - \left(X_{N2} * \beta_{N2,initial} * n_w\right) \quad (6)$$

We calculated the change in N_2 contained in soil air, $\Delta n_{N2,a}$, using Eqn. (7) where T_{STP} is the temperature at STP, 273.15 K; and $T_{initial}$ (K) is the average initial soil temperature from the five thermocouples weighted by soil depth:

$$\Delta n_{N2,a} = \left(\frac{X_{N2} * n_a * T_{STP}}{T_{initial}}\right) - \Delta n_{N2,w} \quad (7)$$

We scaled $\Delta n_{N2,a}$ to the volume of soil beneath the chamber, $\Delta n_{N2,a*}$, using Eqn. (8), where A is the basal area of the chamber in m^2 and z is the soil depth in m:

$$\Delta n_{N2,a*} = \Delta n_{N2,a} * A * z \quad (8)$$

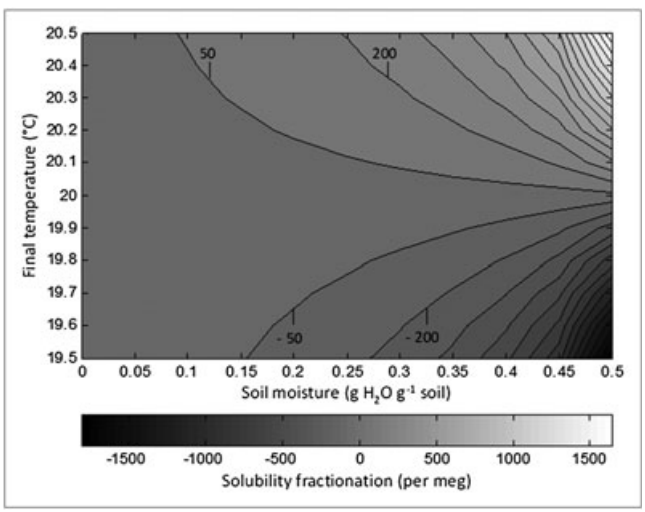

Figure 2. Isolines and shading represent the solubility fractionation effect (in per meg units of δAr/N_2) as a function of soil moisture (g H_2O g^{-1} soil) and a change in soil temperature (°C) from an initial value of 20.0 °C.

We calculated the initial amount of N_2 in the chamber headspace, $n_{N2,c,\ initial}$ in m^3 STP, using Eqn. (9) where V is the chamber volume in m^3:

$$n_{N2,c,initial} = \left(\frac{V * T_{STP}}{T_{initial}}\right) * X_{N2} \quad (9)$$

We then determined the final amount of N_2 in the chamber headspace, $n_{N2,c,final}$ in m^3 STP, using Eqn. (10):

$$n_{N2,c,final} = n_{N2,c,initial} + \Delta n_{N2,a*} \quad (10)$$

We performed the same calculations for Ar to determine $n_{Ar,c,initial}$ and $n_{Ar,c,final}$ in m^3 STP. The dry air mole fraction of Ar was 0.009340 m^3 STP Ar m^{-3} STP.[38]

We estimated the initial Ar/N_2 ratio, in per meg, using Eqn. (11):

$$\left(\delta\frac{Ar}{N_2}\right)_{initial} = \left\{\left[\frac{n_{Ar,c,initial}}{n_{N2,c,initial}} \Big/ \frac{X_{Ar}}{X_{N2}}\right] - 1\right\} * 10^6 \quad (11)$$

We performed the same calculation for the final Ar/N_2 ratio and determined the solubility fractionation effect as the difference between the final and initial Ar/N_2 ratios in units of per meg.

Water vapor flux fractionation

Water vapor flux fractionation occurs when evaporation causes air to diffuse into the soil to replace the water vapor lost; N_2 is a lighter molecular than Ar so the N_2/Ar ratio decreases in response to evaporation.[39] This effect is smaller in environments with low soil evaporation rates. The water vapor flux fractionation effect can be limited to less than 100 per meg if the relative humidity changes from initial value of 95% to a final value of 100% with no accompanying changes in temperature (Fig. 3). Even if the relative humidity begins and ends at 100%, up to a 0.5 °C change in temperature can result in up to a 48 per meg shift in the N_2/Ar ratio because saturation vapor pressure is a function of temperature (Fig. 3).

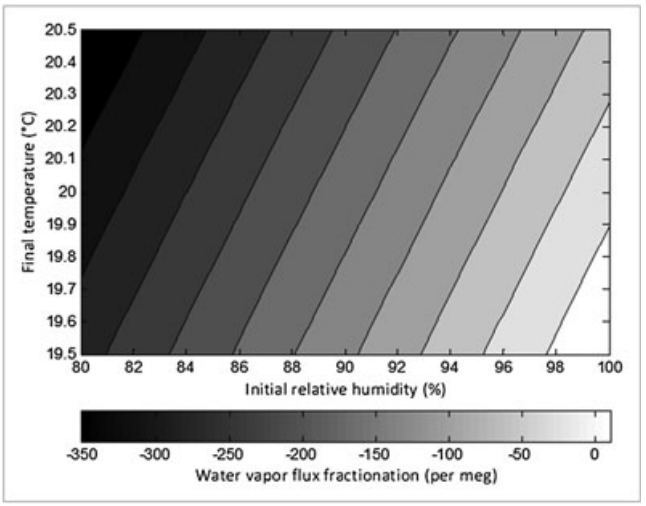

Figure 3. Isolines and shading represent the water vapor flux fractionation effect (in per meg units of $\delta Ar/N_2$) as a function of change in initial relative humidity (%) to a final value of 100% and a change in chamber air temperature (°C) from an initial value of 20.0 °C.

The water vapor flux fractionation effect (per meg), δ_w, can be estimated from the binary diffusion coefficients of gases i and j with water vapor ($D_{i\text{-}H2O}$ and $D_{j\text{-}H2O}$, respectively) and the initial and final water vapor mole fractions (X_{H2O} and X_{H2O}, respectively) according to Severinghaus *et al.*[39] (Eqn. (12)). Gas j is the lighter molecule of the pair, so in this case, j is N_2 and i is Ar. This equation gives the water vapor fractionation effect in terms of Ar/N_2 in per meg:

$$\delta_w = \left[\frac{1 - X_{H2O}}{1 - X_{H2O_0}}^{\left(D_{j-H2O}/D_{i-H2O}\right)-1} - 1\right] * 10^6 \quad (12)$$

The ratio of the binary diffusion coefficients of N_2 and Ar in water vapor was estimated to be 1.0163 using the Fuller method.[40]

The water vapor mole fraction was calculated from water vapor pressure (p_{H2O}, atm) and atmospheric pressure (P, mbar) using Eqn. (13):

$$X_{H2O} = p_{H2O} * \frac{1013.25}{P} \quad (13)$$

The saturation vapor pressure (p_s, atm) was calculated from the measured air temperature (T_{air}, °C) using Eqn. (14):[39]

$$p_{H2Os} = \left[1.69803084 + (0.7568078 * T_{air}) - \left(0.0109724 * T_{air}^2\right) + \left(0.00063967 * T_{air}^3\right)\right] \Big/ 760 \quad (14)$$

The water vapor pressure was then determined from the measured relative humidity (RH, %) and p_s (Eqn. (15)):

$$p_{H2O} = \frac{RH}{100} * p_s \quad (15)$$

Soil surface N_2 flux calculation

Soil surface N_2 fluxes can be calculated from the change in the $\delta Ar/N_2$ values of gas sampled from a surface flux chamber headspace over time. The fundamental assumption of

Rapid Communications in Mass Spectrometry

the N_2/Ar technique is that the headspace Ar concentration remains constant so that changes in $\delta Ar/N_2$ are due solely to changes in the headspace N_2 concentration. For soil surface N_2 fluxes, the physical fractionation effects discussed earlier also cause changes in the $\delta Ar/N_2$ values so these effects must be removed from the measured change in the $\delta Ar/N_2$ values to obtain the biological change in $\delta Ar/N_2$ values The thermal and solubility fractionation effects enhance the measured changes in $\delta Ar/N_2$ values when the temperatures increase and lower measured fluxes in $\delta Ar/N_2$ values when the temperatures decrease. Thus, these effects are subtracted from the measured $\delta Ar/N_2$ value for the final headspace sample. The water vapor flux fractionation effect causes an apparent N_2 flux into the soil, so this effect was added to the measured $\delta Ar/N_2$ value for the final headspace sample. We used the resulting biological $\delta Ar/N_2$ value for the final headspace sample in the following calculations to estimate the actual N_2 flux over the 1-h sampling period.

We determined the N_2 concentration in each sample (mole fraction), c_{sample}, using the following equation where c_{atm} is the atmospheric N_2 concentration (assumed to be 0.78084 mole fraction in air[38]), $\delta Ar/N_2$ is the measured sample value (per meg), and $\delta Ar/N_2$ is the reference standard value (per meg) (Eqn. (16)). The reference standard is La Jolla air sampled from Scripps Pier at the University of California, San Diego (UCSD). The reference standard and samples were analyzed against a working standard consisting of ultra-high-purity (UHP) N_2 and Ar in near atmospheric proportions.

$$c_{sample} = \left\{ \left[\frac{\left(\delta^{Ar}/_{N_2} \right)_{sample}}{1000} \right] + 1 \Big/ \left[\frac{\left(\delta^{Ar}/_{N_2} \right)_{ref}}{1000} \right] + 1 \right\} * C_{atm} \quad (16)$$

The soil surface N_2 flux (mg N m^{-2} day^{-1}), F, was calculated as the linear change in N_2 concentration in the chamber headspace between the two time points using the following equation where m_{N2} is the molecular weight of N_2 (g mol^{-1}), t is the time elapsed (days), and R is the ideal gas constant (8.2057 * 10^{-5} m^3 atm K^{-1} mol^{-1}) (Eqn. (17)):

$$F = \left[(c_{final} - c_{initial}) * V * m_{N2} * 10^3 \right] \Big/ a * t * \frac{P}{R * T_{air}} \quad (17)$$

LABORATORY TEST

Experimental design

We tested the N_2/Ar method by inducing known N_2 fluxes in a diffusion box located in a climate-controlled laboratory at the UCSD. The box consisted of 61 × 61 cm mirror-finished aluminum sheets welded together to leave an open top. A 10.2 cm tall perforated aluminum platform was placed in the diffusion box to create a void space in the bottom. The platform was lined with window screening to minimize sand falling through into the void space. Two 50 × 50 mm fans were mounted on opposite sides of the diffusion box and offset from the center to promote air circulation within the void space. A septum port was installed in the center of a third side to allow injection of N_2 into the void space. The box was filled with air-dried Felton sand (American Soil and Stone, Richmond, CA, USA) to 30 cm depth.

We performed ten consecutive control measurements of N_2 fluxes in dry sand (no N_2 injected) as well as ten consecutive measurements with 2 mL UHP N_2 injected. We also performed ten consecutive measurements of N_2 fluxes in wet sand with no N_2 injected and five consecutive measurements with 10 mL UHP N_2 injected. After each measurement with N_2 injections, we opened the septum port and waited at least 20 h before performing the next measurement. To wet the sand, we added 20 L deionized water to the diffusion box to bring the soil moisture to 10% gravimetric water content. Lysimeters containing 400 g wet sand were used to monitor changes in soil moisture daily. Typically, 1 L deionized water was added every other day to maintain the soil moisture. The sand was mixed to create homogeneous soil moisture throughout the diffusion box, and it was then allowed to equilibrate for at least 12 h before the next measurement. After each flux measurement, triplicate 30-g samples of sand were removed from the diffusion box to determine the gravimetric water content.

The expected N_2 flux induced by the injection of N_2 into the bottom void space of the diffusion box was calculated using Fick's law (Eqn. (18)), where D_s is the soil diffusivity of N_2 (m^2 s^{-1}), dc is the difference in N_2 concentration between the top and bottom of the soil column (mole m^{-3}), and dz is the height of the soil column (m):

$$F = D_s \frac{dc}{dz} \quad (18)$$

Unit conversions are required to obtain F in units of mg N m^{-2} day^{-1}. The soil diffusivity of N_2 was estimated as the product of the free air diffusivity of N_2 and soil tortuosity. The free air diffusivity of N_2 at 20 °C, the ambient air temperature in the laboratory, was 1.92 * 10^{-5} m^2 s^{-1} according to the Fuller equation.[40] Soil tortuosity, τ (unitless), was described using the Millington and Quirk[41] model where f_a is air-filled porosity (m^3 air-filled voids m^{-3} soil) and P_T is total soil porosity (m^3 voids m^{-3} soil) (Eqn. (19)):

$$\tau = \frac{f_a^{10/3}}{P_T^2} \quad (19)$$

Sample collection

Gas samples were collected from a custom-made two-piece 18-L aluminum chamber covered with two layers of reflective bubble wrap. Two internal mixing fans (50 × 50 mm) were attached to the chamber lid. The lid also had inlet and outlet ports consisting of stainless steel Swagelok bulkhead tube fittings sealed on viton. The lip of the chamber lid sealed against a viton strip lining the 1.5" wide lip of the chamber base when clamped together using either six spring clamps or four bar clamps. The chamber was deployed over water and leak checked with SF_6; the measured leak rate over 3 h was 0.3% per hour.

Gas samples were stored in custom-made 2-L cylindrical glass flasks with two parallel 9-mm (o.d.) high-vacuum

valves (Louwers, Hapert, The Netherlands) on one end. The outlet valve was centered on the end of the flask with a glass tube protruding inside almost to the bottom of the flask; the inlet valve was off-centered and connected to a third valve to create a pipette of approximately 1.5 mL volume (Fig. 4). The viton o-rings on the valves were regularly cleaned of lint and other particles, and greased sparingly with high-vacuum lubrication (TorrLube, Santa Barbara, CA, USA). The valves were leak checked on the vacuum line after maintenance. To leak check, a bellows-sealed valve between the turbo pump and the vacuum line was closed for 1 min, and the vacuum line pressure was monitored using a high-vacuum pressure gauge. A change in pressure of $< 10^{-4}$ torr was not considered to be a significant leak.

The chamber, flasks, and a pumping module were connected using ¼" Dekabon tubing attached with stainless steel Swagelok and Ultra-torr fittings. A stainless steel bellows-sealed valve (SS-4H-TH3; Swagelok, Solon, OH, USA) was placed between the inlet and outlet valves for the first flask. Thus, when the bellows-sealed valve was closed, all the sample flask valves were opened to allow flow through both flasks. When the bellows-sealed valve was opened, only the second sample flask valves were open so that the first flask was bypassed. To sample, the flask valves were opened wide so as not to restrict flow. The pump and chamber fans were then turned on for 10 min. A flow meter was used to ensure that the flow rate was at least 4 L min^{-1}. The flasks valves were also closed between samplings. The chamber was first sampled with gas circulating between both flasks and the chamber. After 1 h, the chamber headspace was circulated using only the second flask.

Fractionation during sampling can introduce large biases into N_2/Ar measurements, so a number of precautions were taken. The pump was placed downstream of the flasks so that gas fractionated by the pump would not be directly sampled. Long lengths (2–4 m) of Dekabon tubing were coiled in a horizontal orientation so that any fractionation caused by the pump was separated from the flask. This also helped to minimize gravitational fractionation. Furthermore, the flask valves were closed 5 s after the pump was turned off so that fractionation due to turbulence would be minimized. Lastly, the flask valves were closed very quickly by rolling them with the palm of the hand instead of finger-turning them. This minimizes the fractionation that occurs when a small orifice is left before the valve is completely closed.

Figure 4. Photograph of sample flask valves.

For each measurement, we inserted the chamber base 3 cm into the sand in the center of the box and then inserted T-type thermocouples to five depths (0, 5, 10, 15, 26 cm) next to the chamber. The thermocouples were connected to a CR10X datalogger (Campbell Scientific, Logan, UT, USA) that recorded temperature every 30 s. We turned on the void fans just before injecting the desired amount of UHP N_2 through the septum port using a polypropylene syringe equipped with a zero-volume stopcock. We allowed the void air to continue circulating for 5 min while placing the lid on the chamber base and sealing the chamber. We then turned off the void fans, turned on the chamber fans, and started sampling using the pumping module. We measured the initial relative humidity by placing a thermohygrometer probe (Oakton, Vernon Hills, IL, USA) on the sand surface next to the chamber while the initial gas sample was taken, and we measured the final relative humidity by quickly placing the probe inside the chamber after the final gas sample was taken.

Sample preparation

Gas samples were prepared for mass spectrometric analysis on a vacuum line using a method developed for the Ar/N_2 analysis of gas bubbles trapped in ice core samples.[31] The stainless steel vacuum line included a series of traps: (1) a glass U-trap in ethanol/liquid N_2 mix to −90 °C to remove water vapor, (2) a glass U-trap in liquid N_2 to remove N_2O, carbon dioxide, and hydrocarbons, (3) copper (Cu) mesh in a 5 cm long quartz tube heated to 500 °C to remove O_2, and (4) a glass U-trap in liquid N_2 to remove any hydrocarbons produced in the Cu oven. The Cu was regenerated after every 4–8 samples by passing hydrogen through the heated Cu oven at greater than 5 Torr pressure for 5–10 min.

The sample flask was placed horizontally in the center of an isothermal box with a small opening to allow a ¼" stainless steel tube to protrude to the exterior of the box. This tube connected the flask side port to the end of the vacuum line via Ultra-torr fittings. The flask pipette was pumped down until enough water vapor was removed to leak check the vacuum line. If no leaks were detected, a sample aliquot was transferred from the sample flask to the pipette by closing the vertical valve and then opening the horizontal valve to the flask side port. The gas was allowed to equilibrate for 30 min before the horizontal valve was closed to seal off the bulk sample in the flask.

Sample aliquots were quantitatively transferred from the sample flask pipette to an evacuated dip tube cooled in a liquid helium Dewar. To transfer the aliquot, the vertical valve was opened very slowly to keep the pressure in the vacuum line below 1 Torr; this ensured that all the O_2 in the sample was removed in the Cu oven. The leak check procedure was also used to determine that the entire sample had been transferred into the dip tube and that no leaks had occurred during the transfer. Samples were then allowed to homogenize in the dip tubes for 2–18 h before analysis on the mass spectrometer. As a precaution against variability in measured N_2/Ar ratios caused by differences in

Rapid Communications in Mass Spectrometry

homogenization times, all samples for a given flux measurement were homogenized for a similar amount of time (i.e., no greater than 4 h difference in homogenization time).

Sample analysis

Samples were analyzed on a dual inlet ThermoFinnigan DeltaPlus XP isotope ratio mass spectrometer (Bremen, Germany) with multiple collectors for N, Ar, and O isotopes. Samples containing O_2 are normally analyzed on this instrument, but, during this study, no O_2 was introduced into the mass spectrometer. Samples were analyzed for 6 blocks of 16 cycles using a 12-s integration window. At the beginning of each block, the bellows were compressed to achieve a 4.2 V *m/z* 36 signal to minimize potential errors due to non-linearity. The mass spectrometer output was corrected for pressure imbalance between the two bellows using a linear regression equation based on the 6 block averaged data. For the flux calculations, we used the average Ar/N_2 ratio of 2–3 analytical replicates from each flask.

A working standard gas consisting of high-purity N_2 and Ar in near atmospheric proportions was standardized against La Jolla air collected from the Scripps Pier (La Jolla, CA, USA).[42,43] An aliquot of gas was transferred from the standard can to a stainless steel pipette (bracketed by 4H bellows valves) that had been pumped down online. The gas was allowed to equilibrate between the standard can and the pipette for 20 min before the inner valve was closed; the outer valve was then opened to fill the evacuated standard bellows. Meanwhile, the closed dip tube containing the prepared sample was pumped down online for at least 1 h, and the dip tube was then opened to fill the evacuated sample bellows. The sample and standard are allowed to equilibrate in the completely expanded bellows for 10 min. The standard can, dip tube, and bellows were contained in an isothermal box to minimize N_2/Ar fractionation due to thermal diffusion[44] as well as variability in measured N_2/Ar due to temperature changes during bellows equilibration and/or sample analysis.

We evaluated the external precision of the $\delta Ar/N_2$ measurements by calculating the pooled standard deviation for all analytical replicates within each treatment (e.g., N_2 injected in dry sand). The flux measurements in dry sand with an induced N_2 flux were performed with samples analyzed in triplicates whereas the samples for the other treatments were analyzed in duplicate. The use of duplicates rather than triplicates allowed us to analyze samples for two flux measurements each day rather than only one per day.

RESULTS AND DISCUSSION

Precision and detection limit

We consistently measured N_2/Ar ratios with very high precision. For the flux measurements in dry sand with an induced N_2 flux, the precision was 5 per meg for triplicate sample analysis. For the other treatments, the precision ranged from 12 to 13 per meg for duplicate sample analysis. The poorest reproducibility among analytical replicates for all samples was a standard deviation of 42 per meg for a duplicate set. There were no indications of leaks or other reasons for the poor reproducibility of some replicates, so none of the data were rejected. Despite the higher precision yielded by analyzing triplicates, time constraints forced us to analyze duplicates for most of the flux measurements performed. This allowed us to approximately double our throughput, analyzing samples for two flux measurements per 14-h work day versus one flux measurement per 12-h work day. Using our sampling equipment and procedure, a 1 per meg change in $\delta Ar/N_2$ was equivalent to an N_2 flux of approximately 3 mg N m^{-2} day^{-1}. If the detection limit of the method is calculated as three times the precision in $\delta Ar/N_2$ analysis, the detection limit is 45 mg N m^{-2} day^{-1} using triplicates whereas it is 108 mg N m^{-2} day^{-1} using duplicates.

The correction for the physical fractionation effects on N_2/Ar ratios can create additional errors in the flux measurements if temperature and relative humidity are not accurately measured. These errors would probably overwhelm the errors associated with the models used to estimate the physical fractionation effects. For example, if the chamber temperature was initially 0.1 °C warmer than measured, the thermal fractionation effect would be 28.6 per meg greater and the water vapor flux fractionation effect would be 9 per meg less than measured for a total underestimate of 19.6 per meg for these fractionation effects. This would translate to a 78 mg N m^{-2} day^{-1} error in the corrected N_2 flux.

Measurements in dry sand

The control measurements in dry sand demonstrate that flux values below the calculated detection limit of 108 mg N m^{-2} day^{-1} are highly variable and can be inaccurate. For three of the ten measurements, we observed a 1 per meg change in $\delta Ar/N_2$, which is consistent with no induced N_2 flux. However, overall we measured changes in $\delta Ar/N_2$ ranging from −71 to 18 per meg corresponding to an average N_2 flux of 43 ± 27 mg N m^{-2} day^{-1} (± SE, n = 10). When corrected for thermal fractionation, which ranged in magnitude from 19 to 96 per meg, the N_2 flux was 46 ± 45 mg N m^{-2} day^{-1}. This could suggest that the sampling protocol causes an artifact of approximately 45 mg N m^{-2} day^{-1}. However, the average measured N_2 flux of 111 ± 19 mg N m^{-2} day^{-1} (n = 10) closely matched an induced N_2 flux of 108 mg N m^{-2} day^{-1} in dry sand. Therefore, the control measurements probably do not represent a sampling artifact but simply reflect our inability to accurately measure N_2 fluxes below the detection limit.

The induced N_2 flux measurements in dry sand suggest that thermal fractionation may not be manifested within the 1-h sampling period that we used. In dry soil, solubility and water vapor flux fractionation do not occur, allowing us to separately test thermal fractionation effects. The measured changes in $\delta Ar/N_2$ ranged from −59 to 2 per meg while the thermal fractionation effect ranged from −34 to 34 per meg. When thermal fractionation was taken into account, the average corrected N_2 flux was 91 ± 36 mg N m^{-2} day^{-1}. The correction for thermal fractionation not only caused the measured N_2 flux to diverge from the expected N_2 flux, but it also increased the variability in the measured N_2 fluxes. The coefficient of variation (CV) for the uncorrected N_2 fluxes was 53% whereas the CV for the

corrected N_2 fluxes was 124%. This suggests that the correction for thermal fractionation does not improve the N_2 flux estimation and does not accurately represent the effects of thermal diffusion on the N_2/Ar ratio. For these reasons we do not recommend the use of a thermal fractionation correction for measurements on short time scales.

There are several reasons why the correction for thermal fractionation may not be valid or necessary for our N_2 flux measurements. First, changes in the temperature differential between the chamber headspace and soil depth were ≤0.3 °C. Although thermal fractionation causes a 286 per meg shift in $\delta Ar/N_2$ per degree of temperature change, it is possible that small changes in the temperature gradient within 1 h do not cause a detectable shift in the $\delta Ar/N_2$ of the chamber headspace gas. Second, where thermal fractionation has been observed – in sand dunes, polar firn, and ice cores – the gases had reached steady-state equilibria.[39,42,45] In the diffusion box, thermal steady-state conditions were not reached because the temperature changed throughout the sampling period, violating a fundamental assumption of the thermal diffusion correction. Thus, it is possible that thermal fractionation may not have been manifested because the gas molecules had not reached equilibrium with respect to the temperature gradient in the sand. Third, the temperature profiles show that the temperature change was often non-linear with depth, making it difficult to model a shift in the $\delta Ar/N_2$ values of the chamber headspace due to thermal fractionation. Here we simply assumed a linear temperature gradient between the chamber headspace and the bottom of the diffusion box to calculate the thermal fractionation effect. This simplified approach may not have been valid.

Measurements in wet sand

When we wet the diffusion box sand to 10% gravimetric soil water content, we observed evidence of the water vapor flux fractionation effect, which causes a decrease in the N_2/Ar ratio to create an apparent net uptake of N_2 by the soil. For the control measurements, we observed N_2 fluxes of -45 ± 82 mg N m^{-2} day^{-1} (n = 5) when the water vapor flux fractionation effect was not taken into account. We also performed these flux measurements after allowing for an initial 10-min period with the chamber lid set but not sealed on the chamber base before the sampling procedure began. This additional time would be needed for the added N_2 to move through the wet sand for the induced N_2 flux measurements. This change in procedure did not significantly change the measured N_2 fluxes, with a measured N_2 flux of -48 ± 78 mg N m^{-2} day^{-1} (n = 5). We used this modified sampling protocol for flux measurements with a known N_2 flux of 160 mg N m^{-2} day^{-1} (from the injection of 10 mL UHP N_2) in wet sand; the measured N_2 flux was 62 ± 25 mg N m^{-2} day^{-1}. As expected, the measured N_2 fluxes were lower than the expected N_2 fluxes for all treatments when the water vapor flux fractionation effect was not considered.

The water vapor flux fractionation effect was difficult to quantify because the thermohygrometer readout took approximately 5 min to stabilize, and, during this time, the relative humidity inside the chamber was changing in response to ongoing evaporation. The measurement was also complicated by the fact that we could not place the thermohygrometer probe inside the chamber during the flux measurement due to the design of the chamber. Measurements of changes in relative humidity inside the chamber taken when gas was not being sampled show that the relative humidity reached 98.8% in 10 min and 99.4% in 20 min after the chamber lid was placed on the deployed chamber base. Assuming that the initial air inside connecting tubing and the flasks was at ambient relative humidity (50%) and that the chamber headspace was at 99.9% relative humidity, we calculate a relative humidity of 90% at the initial time point, and an assumed relative humidity of 99.9% at the final time point. A 1% error in relative humidity translates into a 15 per meg error in the water vapor flux fractionation effect.

Solubility fractionation had a relatively small effect on $\delta Ar/N_2$ compared with the other fractionation effects. With the assumed relative humidity and measured air temperature, we estimated that the water vapor flux fractionation effect ranged from 28 to 42 per meg for all the measurements in wet sand, the solubility fractionation effect ranged from −17 to 15 per meg, and the thermal fractionation effect ranged from −64 to 32 per meg. We calculated solubility fractionation based on the average soil temperature. If the solubility fractionation effect was calculated for each depth increment and then summed, it only produced a 1 per meg difference compared with the approach that we used. With the relatively low soil moisture in the diffusion box and the small temperature changes during our flux measurements, the solubility fractionation effect was only −17 to 15 per meg, with the direction of the effect dependent on whether the bulk soil cooled or warmed during the measurement. This effect could be larger when soil moisture is higher or when temperature changes are greater. For example, Fig. 2 shows that at 40% gravimetric soil water content, the solubility fractionation effect is greater than 100 per meg per 0.1 °C change in temperature. This underscores the importance of limiting temperature changes during N_2/Ar measurements, which can be accomplished by shading the chamber and avoiding the times of day with large changes in soil temperature (e.g., just after sunrise).

The flux measurements in wet sand support the implications from the flux measurements in dry sand. For the control measurements, the average measured N_2 flux corrected for all physical fractionation factors was 86 ± 45 mg N m^{-2} day^{-1} whereas the average N_2 flux was 67 ± 68 mg N m^{-2} day^{-1} when only corrected for solubility and water vapor flux fractionation. These measurements demonstrate that we cannot measure N_2 fluxes below the calculated detection limit. For the induced N_2 flux measurements, the average N_2 flux was 134 ± 38 mg N m^{-2} day^{-1} when all physical fractionation effects were accounted for and 146 ± 20 mg N m^{-2} day^{-1} when only solubility and water vapor flux fractionation were considered. Without correcting for thermal fractionation, the average measured N_2 flux was more similar to the expected N_2 flux of 160 mg N m^{-2} day^{-1} and also less variable. Thus, this provides additional evidence that the correction for thermal fractionation is not useful as currently implemented.

Water vapor flux fractionation was the most poorly constrained physical fractionation effect, but we were able to effectively account for its effect on the N_2/Ar ratio. Our approximation of the initial relative humidity in the chamber headspace appears to be valid because the measured N_2 fluxes corrected for the water vapor flux and solubility fractionation effects agreed well with the expected values for

Rapid Communications in Mass Spectrometry

the induced N_2 fluxes. However, it is preferable for water vapor pressure to be measured in the chamber headspace in real time with an instrument that stabilizes more quickly.

We tested the N_2/Ar technique in sand, but we expect that in general the physical fractionation effects on soils with finer textures will be similar. However, in clayey soils with very small pore spaces, gas diffusion is characterized by Knudsen diffusion in which gas molecules are more likely to collide with soil grains than with other gas molecules.[46] The addition of a Knudsen diffusion term would complicate the modeling of water vapor flux fractionation as presented here.[39]

Future improvements to the method

The detection limit for this method at present is very high, but it can easily be lowered proportionally by increasing the ratio of chamber basal area to volume as well as by increasing the sampling time period. For example, doubling the ratio of chamber basal area to volume or the sampling time period would lower the detection limit by 50%. Chambers with large basal areas can be unwieldy and difficult to deploy in ecosystems with dense vegetation. Theoretically, the ratio of chamber basal area to volume can also be increased by decreasing the chamber height from the 12 cm that we used. Short chambers (<10 cm tall) can suppress soil surface trace gas fluxes because of gas storage in the soil surface.[47] A longer sampling time period can also lower the detection limit, but, like short chambers, it can cause changes in the concentration gradients of trace gases in the soil and suppress the surface flux. While N_2 is not a trace gas, changes in the diffusion of trace gases could cause corresponding non-trivial changes in N_2 diffusion. Thus, these measures for lowering the detection limit should be employed with caution.

The N_2/Ar technique can be applied to soil depth profiles which may exhibit greater differences in N_2-Ar that can be measured accurately using the gas analysis approach described here. This approach creates the challenge of sampling soil gas without causing fractionation at the per meg level. We have attempted passive sampling in laboratory tests with no induced change in N_2, but we have measured approximately 500 per meg fractionation in δAr/N_2 (data not shown). Additional investigation is necessary to understand the cause of this fractionation. The sampling procedure that we used in this study involved pumping air through large-volume flasks and resulted from many years of testing to minimize sampling artifacts associated with this approach. For example, Blaine *et al.*[43] found that temperature gradients within the sampling equipment can cause N_2/Ar fractionation. Another factor in using the soil profile approach is the sample volume of soil gas that can be collected. A large sample volume is required for running analytical replicates without fractionating the remaining sample in the flask. If analytical replicates are not desired, entire small samples could be analyzed to avoid fractionation. Beyond these practical considerations, the physical fractionation effects will also need to be constrained along the soil profile. At steady state, solubility fractionation will not affect the observed soil air N_2/Ar gradient through the soil profile. However, the thermal and water vapor flux fractionation effects will affect the observed N_2/Ar soil profile under both steady-state and transient conditions. Thus, constraining the physical effects on N_2/Ar gradients in soil air differs from constraining the physical effects on the N_2/Ar ratio in the headspace of surface flux chambers, which is subject only to the transient aspects of the fractionating processes.

Theoretically, the observed fractionation of inert gas ratios or isotope ratios of inert gases can be used to constrain the physical fractionation effects on N_2-Ar. For example, δ^{40}Ar and δ^{15}N values are often used together in paleoclimate work to separate different physical fractionation effects.[45] Argon is the most abundant naturally occurring inert gas, and the isotopic composition of Ar can be measured with higher precision than that of other inert gases. However, the precision for Ar isotopic analysis is lower than that for δAr/N_2 so it cannot be used to accurately constrain physical fractionation effects on N_2-Ar. Future improvements in δ^{40}Ar analysis could allow this approach to be used as validation of the modeling approach that we employed to estimate the physical fractionation effects.

Gas analysis using a dual inlet IRMS instrument with offline sample preparation had a very low throughput that precludes its use for high-resolution measurements of soil N_2 emissions. This analytical approach was chosen for this study because the instrumentation and protocols were already set up and tested for our analyses. Keeling *et al.*[48] presented a higher throughput method on a continuous flow IRMS system with online removal of water vapor and carbon dioxide that provides δAr/N_2 analysis with per meg level precision similar to that presented here. The addition of online O_2 removal would permit their method to be applied to our approach. With a higher throughput method, the analysis of more replicates per sample could lower the detection limit considerably. For example, we observed 5 per meg precision for δAr/N_2 values when analyzing analytical triplicates and 12 per meg precision when analyzing analytical duplicates. Thus, the detection limit would be lowered from 108 mg N m^{-2} day^{-1} to 45 mg N m^{-2} day^{-1} simply by analyzing analytical triplicates instead of duplicates. Furthermore, gas handling from offline sample preparation probably introduces a large proportion of the variability among analytical replicates and, as such, online sample preparation would probably improve the external precision. It could be possible to achieve 1 per meg precision, which would yield a detection limit of 3 mg N m^{-2} day^{-1}. This is comparable with the detection limit reported for the gas flow core method[14] and the ^{15}N gas flux method.[11] Thus, a continuous flow IRMS approach could not only increase sample throughput, but also lower the detection limit of the method so that it can be used in ecosystems with low soil N_2 emissions

CONCLUSIONS

We demonstrated that the N_2/Ar technique can be used to measure soil N_2 emissions without manipulating soil conditions. Given the current high detection limit and throughput limitations of the method, it is currently best suited as a verification tool for other methods in ecosystems with high soil N_2 emissions rather than a technique for high-resolution field measurements. Physical fractionation effects on the N_2/Ar ratio can be constrained, but accurate measurements of temperature and relative humidity are necessary. Moreover,

temperature changes and evaporation during the sampling period should be minimized to limit the physical fractionation effects. With technological and methodological advances we can lower the detection limit, better constrain the physical fractionation effects, and increase sample throughput so that the N_2/Ar technique can be used in a wider range of ecosystems for high resolution field measurements of soil N_2 emissions.

SUPPORTING INFORMATION

Additional supporting information may be found in the online version of this article.

Acknowledgements

We appreciate comments from three anonymous reviewers and J. P. Severinghaus that improved this manuscript. We also thank J. P. Severinghaus for use of his IRMS facility and helping us model the physical fractionation effects. We appreciate training and troubleshooting assistance from R. Beaudette, V. Petrenko, M. Headly, A. Orsi, and T. Kobashi. This research was funded by a US National Science Foundation (NSF) grant (DEB-0842385) to W.L.S. as well as an NSF Doctoral Dissertation Improvement Grant (0808383) and a Berkeley Atmospheric Sciences Center Graduate Research Fellowship to W.H.Y. W.H.Y. was supported by a Department of Energy Global Change Education Program Graduate Research Environmental Fellowship and subsequently by a NSF Graduate Research Fellowship.

REFERENCES

[1] A. Tietema, J. M. Verstraten. Nitrogen cycling in an acid forest ecosystem in the Netherlands under increased atmospheric nitrogen input - the nitrogen budget and the effect of nitrogen transformations on the proton budget. *Biogeochemistry* **1991**, *15*, 21.
[2] L. O. Hedin, P. M. Vitousek, P. A. Matson. Nutrient losses over four million years of tropical forest development. *Ecology* **2003**, *84*, 2231.
[3] P. M. Groffman, M. A. Altabet, J. K. Bohlke, *et al*. Methods for measuring denitrification: diverse approaches to a difficult problem. *Biogeochemistry* **2006**, *16*, 2091.
[4] W. H. Schlesinger. On the fate of anthropogenic nitrogen. *Proc. Natl. Acad. Sci. USA* **2009**, *106*, 203.
[5] P. M. Vitousek, J. D. Aber, R. W. Howarth, *et al*. Human alteration of the global nitrogen cycle: Sources and consequences. *Ecol. Appl.* **1997**, *7*, 737.
[6] J. N. Galloway, J. D. Aber, J. W. Eriseman, *et al*. The nitrogen cascade. *Bioscience* **2003**, *53*, 341.
[7] P. M. Groffman. Nitrogen balances at ecosystem, landscape, regional and global scales, in *Nitrogen in Agricultural Soils*, (Eds: J. Schepers, W. Raun). Soil Science Society of America, Madison, WI, **2008**.
[8] E. W. Boyer, R. B. Alexander, W. J. Parton, *et al*. Modeling denitrification in terrestrial and aquatic ecosystems at regional scales. *Ecol. Appl.* **2006**, *16*, 2123.
[9] R. Knowles. Acetylene inhibition technique: development, advantages, and potential problems, in *Denitrification in Soil and Sediment*, (Eds: N. Revsbech, J. Sørensen). Plenum Press, New York, **1990**, pp. 151–166.
[10] T. Simarmata, G. Benckiser, J. C. G. Ottow. Effect of an increasing carbon:nitrate-N ratio on the reliability of acetylene in blocking the N_2O-reductase activity of denitrifying bacteria in soil. *Biol. Fertil. Soils* **1993**, *15*, 107.
[11] R. J. Stevens, R. J. Laughlin. Measurement of nitrous oxide and dinitrogen emissions from agricultural soils. *Nutr. Cycling Agroecosyst.* **1998**, *52*, 131.
[12] K. Butterbach-Bahl, R. Gasche, G. Willibald, H. Papen. Exchange of N-gases at the Hoglwald Forest – A summary. *Plant Soil* **2002**, *240*, 117.
[13] M. Dannenmann, K. Butterbach-Bahl, R. Gasche, G. Willibald, H. Papen. Dinitrogen emissions and the N_2:N_2O emission ratio of a Rendzic Leptosol as influenced by pH and forest thinning. *Soil Biol. Biochem.* **2008**, *40*, 2317.
[14] K. Butterbach-Bahl, G. Willibald, H. Papen. Soil core method for direct simultaneous determination of N_2 and N_2O emissions from forest soils. *Plant Soil* **2002**, *240*, 105.
[15] T. J. Chestnut, D. J. Zarin, W. H. McDowell, M. Keller. A nitrogen budget for late-successional hillslope tabonuco forest, Puerto Rico. *Biogeochemistry* **1999**, *46*, 85.
[16] C. Scheer, R. Wassmann, K. Butterbach-Bahl, J. Lamers, C. Martius. The relationship between N_2O, NO, and N_2 fluxes from fertilized and irrigated dryland soils of the Aral Sea Basin, Uzbekistan. *Plant Soil* **2009**, *314*, 273.
[17] M. K. Firestone, R. B. Firestone, J. M. Tiedje. Nitrous oxide from soil denitrification: Factors controlling its biological production. *Science* **1980**, *208*, 749.
[18] K. L. Weier, J. W. Doran, J. F. Power, D. T. Walters. Denitrification and the dinitrogen nitrous-oxide ratio as affected by soil-water, available carbon, and nitrate. *Soil Sci. Soc. Am. J.* **1993**, *57*, 66.
[19] B. Z. Houlton, D. M. Sigman, L. O. Hedin. Isotopic evidence for large gaseous nitrogen losses from tropical rainforests. *Proc. Natl. Acad. Sci. USA* **2006**, *103*, 8745.
[20] B. Z. Houlton, E. Bai. Imprint of denitrifying bacteria on the global terrestrial biosphere. *Proc. Natl. Acad. Sci. USA* **2009**, *106*, 21713.
[21] W. H. Yang, Y. A. Teh, W. L. Silver. A test of a field-based ^{15}N-nitrous oxide pool dilution technique to measure gross N_2O production in soil. *Global Change Biol.* **2011**. DOI: 10.1111/j.1365-2486.2011.02481.x.
[22] T. Dalsgaard, B. Thamdrup. Factors controlling anaerobic ammonium oxidation with nitrite in marine sediments. *Appl. Environ. Microbiol.* **2002**, *68*, 3802.
[23] C. J. Schubert, E. Durisch-Kaiser, B. Wehrli, B. Thamdrup, P. Lam, M. M. M. Kuypers. Anaerobic ammonium oxidation in a tropical freshwater system (Lake Tanganyika). *Environ. Microbiol.* **2006**, *8*, 1857.
[24] J. J. Rich, O. R. Dale, B. Song, B. B. Ward. Anaerobic ammonium oxidation (Anammox) in Chesapeake Bay sediments. *Microb. Ecol.* **2008**, *55*, 311.
[25] M. S. M. Jetten, L. van Niftrik, M. Strous, B. Kartal, J. T. Keltjens, H. J. M. Op den Camp. Biochemistry and molecular biology of anammox bacteria. *Crit. Rev. Biochem. Mol. Biol.* **2009**, *44*, 65.
[26] C. R. Penton, A. H. Devol, J. M. Tiedje. Molecular evidence for the broad distribution of anaerobic ammonium-oxidizing bacteria in freshwater and marine sediments. *Appl. Environ. Microbiol.* **2006**, *72*, 6829.
[27] S. Humbert, S. Tarnawski, N. Fromin, M. Mallet, M. Aragno, J. Zopfi. Molecular detection of anammox bacteria in terrestrial ecosystems: distribution and diversity. *ISME J.* **2010**, *4*, 450.
[28] W. H. Yang, K. A. Weber, W. L. Silver. Nitrogen loss from soil via anaerobic ammonium oxidation coupled to iron reduction. *Nature* **2012**, submitted.

[29] T. M. Kana, C. Darkangelo, M. D. Hunt, J. B. Oldham, G. E. Bennett, J. C. Cornwell. Membrane inlet mass spectrometer for rapid high precision determination of N_2, O_2, and Ar in environmental water samples. *Anal. Chem.* **1994**, *66*, 4166.
[30] S. Seitzinger, J. Harrison, J. K. Bohlke, *et al*. Denitrification across landscapes and waterscapes: A synthesis. *Ecol. Appl.* **2006**, *16*, 2064.
[31] T. Kobashi, J. P. Severinghaus, K. Kawamura. Argon and nitrogen isotopes of trapped air in the GISP2 ice core during the Holocene epoch (0–11,500 B.P.): Methodology and implications for gas loss processes. *Geochim. Cosmochim. Acta* **2008**, *72*, 4675.
[32] J. Kincaid, E. Cohen, M. Lopez de Haro. The Enskog theory for multicomponent mixtures. IV. Thermal diffusion. *J. Chem. Phys.* **1987**, *86*, 963.
[33] S. Chapman, F. Dootson. Thermal diffusion. *Philos. Mag.* **1917**, *33*, 248.
[34] K. Grew, T. Ibbs. *Thermal Diffusion in Gases*. Cambridge University Press, Cambridge, **1952**.
[35] S. Chapman, T. Cowling. *The Mathematical Theory of Non-Uniform Gases*. Cambridge University Press, Cambridge, **1970**.
[36] G. Blake, K. Hartge. Particle density, in *Methods of Soil Analysis. Part 1. Physical and Mineralogical Methods*, (Ed.: A. Klute). Soil Science Society of America, Madison, WI, **1986**, p. 377.
[37] R. C. Hamme, S. R. Emerson. The solubility of neon, nitrogen and argon in distilled water and seawater. *Deep-Sea Res., Part I* **2004**, *51*, 1517.
[38] E. Glueckauf. The composition of atmospheric air, in *Compendium of Meterology*. American Meteorological Society, Boston, **1951**, p. 3.
[39] J. P. Severinghaus, M. L. Bender, R. F. Keeling, W. S. Broecker. Fractionation of soil gases by diffusion of water vapor, gravitational settling, and thermal diffusion. *Geochim. Cosmochim. Acta* **1996**, *60*, 1005.
[40] E. Polling, J. Prausnitz, J. P. O'Connell, *The Properties of Gases and Liquids*, McGraw-Hill, **2001**.
[41] R. Millington, J. P. Quirk. Permeability of porous solids. *Trans. Faraday Soc.* **1961**, *57*, 1200.
[42] J. P. Severinghaus, A. Grachev, B. Luz, N. Caillon. A method for precise measurement of argon 40/36 and krypton/argon ratios in trapped air in polar ice with applications to past firn thickness and abrupt climate change in Greenland and at Siple Dome, Antarctica. *Geochim. Cosmochim. Acta* **2003**, *67*, 325.
[43] T. W. Blaine, R. F. Keeling, W. J. Paplawsky. An improved inlet for precisely measuring the atmospheric Ar/N-2 ratio. *Atmos. Chem. Phys.* **2006**, *6*, 118.
[44] A. M. Grachev, J. P. Severinghaus. Laboratory determination of thermal diffusion constants for N-29(2)/N-28(2) in air at temperatures from −60 to 0 °C for reconstruction of magnitudes of abrupt climate changes using the ice core fossil-air paleothermometer. *Geochim. Cosmochim. Acta* **2003**, *67*, 345.
[45] J. P. Severinghaus, T. Sowers, E. J. Brook, R. B. Alley, M. L. Bender. Timing of abrupt climate change at the end of the Younger Dryas interval from thermally fractionated gases in polar ice. *Nature* **1998**, *391*, 141.
[46] R. B. Bird, W. E. Stewart, E. N. Lightfoot. *Transport Phenomena*. John Wiley, New York, **1960**.
[47] F. Conen, K. A. Smith. An explanation of linear increases in gas concentration under closed chambers used to measure gas exchange between soil and the atmosphere. *Eur. J. Soil Sci.* **2000**, *51*, 111.
[48] R. F. Keeling, T. Blaine, B. Paplawsky, L. Katz, C. Atwood, T. Brockwell. Measurement of changes in atmospheric Ar/N_2 ratio using a rapid-switching, single-capillary mass spectrometer system. *Tellus, Ser. B* **2004**, *56*, 322.

